Spectral structure of 245–445 keV electrons and positrons in positron-thorium scattering

Chr. Bargholtz, L. Holmberg, K. E. Johansson, D. Liljequist,
P.-E. Tegnér, and D. Vojdani
Department of Physics, University of Stockholm, Vanadisvägen 9, S-11346 Stockholm, Sweden
(Received 1 February 1989)

Anomalies in low-energy positron scattering from thorium are searched for. The incident positrons were emitted from a ^{68}Ga source with an end-point energy of 1.90 MeV. Coincidences between electrons and positrons in the energy range 245–445 keV were registered in a double beta spectrometer. The electron and positron energy spectra are best described in terms of Bhabha scattering with a small additional structure at an energy of about 320 keV for both the electrons and the positrons. The significance of this peak is estimated to be three standard deviations. The spectrometer was also used in a study of scattering of electrons emitted in the decay of ^{90}Y, with an end-point energy of 2.28 MeV. The electron-electron coincidence spectrum in the energy range 245–445 keV is well described as resulting from Møller scattering alone.

I. INTRODUCTION

The purpose of this experiment was to investigate the possible existence of a coincident electron-positron peak at a kinetic energy around 330 keV for both the detected particles as claimed by Erb, Lee, and Milner in positron scattering on a thorium foil target.[1] Similar investigations not confirming the results by Erb *et al.* have been reported by Peckhaus *et al.*[2] and Wang *et al.*[3] They studied positron scattering on thorium using miniorange spectrometers. No peak structure was found in these investigations. Positron scattering on low-Z elements has been studied with conflicting conclusions concerning the occurrence of peaks.[4–7] New evidence for structure in the spectrum of electrons resulting in positron scattering on Th and U targets has recently been reported by Sakai *et al.*[8] They used positrons from ^{118}Sn with a maximum kinetic energy of 2.66 MeV. In the singles electron spectra a line of kinetic energy 330.8 keV and a FWHM equal to 3.7±0.5 keV was found.

The experiments mentioned above followed the experimental evidence for narrow positron lines and coincident electron and positron peaks reported in experiments on heavy-ion collisions performed at Gesellschaft für Schwerionenfurschong (GSI) in Darmstadt.[9] A recent investigation of heavy-ion reactions at the SuperHILAC in Berkeley[10] gave evidence for pairs of equal-energy photons, an effect that might be related to the electron-positron peaks seen at GSI. At present no satisfactory theoretical explanation exists for these narrow peaks.

A first account of our work has been published in Ref. 11. Since then the measurements have been extended to include electron-electron coincidence spectra resulting from scattering of electrons on a thorium target. A more general method for analysis of the experimental data has been adopted and the positron scattering data have been reanalyzed accordingly. Beside the new measurements and the result of the reanalysis we present, in greater detail than previously, the experimental method and the calculation of the electron and positron scattering corrections.

The interpretation of the results mentioned above has often involved the existence of new particles, particularly the axion. There is now a large number of proposed light particles introduced to explain some of the unwanted or unseen symmetries of the theory (for a review, see Ref. 12). The originally proposed axion,[13] introduced to solve the problem of charge-parity (CP) violation in strong interactions, is a light pseudoscalar particle with semiweak couplings. Several models have been proposed with the aim to solve the fundamentally important strong CP problem.[14] The correct model must, however, be determined by experiments. To summarize, there are interesting experimental indications and theoretical expectations to warrant a systematic search for anomalous interactions of low-energy positrons.

II. EXPERIMENTAL ARRANGEMENT

We studied the coincident electron-positron spectra and electron-electron spectra that resulted when positrons and electrons, respectively, were scattered on thorium targets. The positrons and electrons were obtained from radioactive sources deposited on the target foils.

A Gerholm magnetic coincidence spectrometer was used for focusing the positrons and electrons (Ref. 15 and references therein). It consists of two iron-capsuled long lenses placed end to end with a common axis (Fig. 1). The magnetic field in the lenses can be varied in order to select particles of appropriate momenta. The positrons and electrons enter the lenses at a mean angle of about 30° relative to the axis. Twisted baffle systems were inserted in both lenses in order to detect only positrons or electrons, respectively. Lead plugs centered around the lens axis prevented gamma radiation and annihilation quanta from passing directly from the source to the plastic scintillators.

The magnetic lenses were energy calibrated by focusing

 ©1989 The American Physical Society

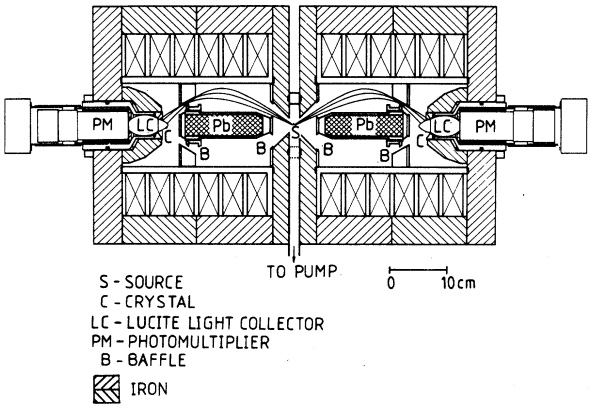

FIG. 1. Schematic layout of the spectrometer. Electron and positron trajectories are shown originating from the source-target foil (S) and being detected by the crystal (C) and photomultiplier (PM) assembly.

on a conversion-electron line in the energy region of interest, namely the 295.9-keV line occurring in the decay of ^{152}Eu. The momentum resolution was determined from the FWHM of the 624.2-keV line in the decay of ^{137}Cs as 7%. The corresponding energy resolution at 345 keV is 40 keV, which is about the same as the energy spread caused by straggling in the thorium foil. The transmission was determined from the accepted number of 624.2-keV electrons, emitted from an intensity calibrated source. With the electron/positron baffles inserted the transmission was about 2%.

Three amplitude to digital converters were used for the analysis of the pulses from the scintillation detectors and from a time to amplitude converter. A full range time window of 100 ns was used and for events falling in this time window both pulse heights as well as the time difference between the events were registered. The time resolution was 0.8 ns (FWHM). Beside these coincidence events a determined fraction of the singles counts were registered. The information about the accepted events was stored on magnetic tape. The data acquisition system is described in Ref. 16.

As a source of positrons we used ^{68}Ga ($T_{1/2}=68.3$ min) which was obtained in the decay of ^{68}Ge ($T_{1/2}=275$ d). A solution of ^{68}Ga in 0.003 molar ethylenediamine tetra-acetic acid (EDTA) was evaporated to dryness on a thorium foil. The gallium source thickness varied in the interval 6–25 mg/cm^2. The thorium foil had been rolled to a thickness of approximately 25 μm (28 mg/cm^2). The activity at the start of a measurement was typically 10 MBq (270 μCi). The number of sources was 32. Measurements were carried out with each source during about 3 h.

The source-target foil was inserted into the spectrometer and centered with respect to the two lenses. Three different arrangements were used:

Geometry 1: The plane of the foil was perpendicular to the axis of the lenses with the side of the foil covered with the source facing the electron detector.

Geometry 2: Same as geometry 1 but with the source side facing the positron detector.

Geometry 3: The plane of the foil was along the lens axis.

The measurements were performed by setting the currents of the electron and positron lenses at fixed values during 400-s intervals. The values chosen form a 5×5 matrix corresponding to electron and positron energies of 265, 305, 345, 385, and 425 keV.

In the study of electron scattering we used a source of ^{90}Sr ($T_{1/2}=28.8$ y) which decays to beta active ^{90}Y. The end-point energy of the electron spectra are 0.55 MeV and 2.28 MeV, respectively. The source had a strength of about 0.2 MBq (5 μCi) and constituted a very thin layer deposited on a 30-μm thorium foil.

The same coincidence spectrometer as for the study of positron scattering was used. In the lens previously used for selecting positrons the direction of the magnetizing current was reversed in order to let electrons pass the baffle. The source-target foil was centered with respect to the lenses and was oriented with its plane perpendicular to the lens axis.

The measurements were performed by setting the currents of the lenses at fixed values with a measurement time of about 50 h for each current combination. As for the positron scattering, the values chosen form a 5×5 matrix corresponding to electron energies of 265, 305, 345, 385, and 425 keV.

III. MONTE CARLO SIMULATIONS

A. Simulation of positron scattering

We have made Monte Carlo studies of electron-positron scattering in the combined gallium source and thorium foil target. The Monte Carlo programs are based on models and procedures described in more detail elsewhere.[17] Two processes were simulated: (i) Bhabha scattering events in the thorium foil and the source material, (ii) hypothetical events involving a positron and an electron starting back to back in the thorium foil with initial energies about 350 keV.

The positrons are emitted in random directions from random sites in a source layer deposited on a 25-μm-thick thorium foil. The positron initial energy is distributed according to a β^+ spectrum where the dominating branch has an end point energy of 1.90 MeV.[18] The positrons undergo deflection and energy loss in the gallium source layer as well as in the thorium foil. The deflection is practically entirely due to multiple elastic scattering. The energy loss is mainly due to atomic excitation and ionization, and to a minor part to radiative loss. The ionization includes Bhabha scattering events, where a positron is scattered by an electron considered initially free and at rest.

The electron and positron stopping power in thorium at energies between 0.2 and 1.90 MeV is typically 1.2–1.6 keV/μm. Since the path length within the thorium foil is of the order of 10–50 μm, energy losses of the order of 10–80 keV are expected. The average deflection per unit path length is conveniently expressed in terms of the transport mean free path λ_{tr}.[19] We are mainly concerned

with energies of the scattered leptons in the range 250–450 keV and initial positron energies of about 500–900 keV. For 350 keV e^+ and e^-, $\lambda_{tr} \approx 12$ μm and consequently their direction of motion is essentially randomized by scattering in the 25-μm-thick thorium foil. At 700 keV, $\lambda_{tr} \approx 35$ μm which means that the "primary" positrons are substantially scattered, but not entirely randomized. This is demonstrated in Fig. 2, which shows the simulated trajectory patterns of 350-keV electrons and 700-keV positrons.

The mass thickness of the source layer, consisting of Ga in an organic substrate, was set to 13 mg/cm^2, which is about 40% of the mass thickness of the thorium foil. Due to the large difference in the effective atomic number, the stopping power per unit mass thickness was estimated to be 1.8 times that in thorium, while λ_{tr}, measured as mass/area, was estimated to be 12 times that in thorium. Therefore the scattering is relatively weak in the source layer, but the energy loss may be comparable to that in the thorium foil. To account for the uncertainties in the thickness and scattering characteristics of the source layer used in the experiment, we performed analyses assuming three different source layer mass thicknesses of 6.4, 13 (the main case) and 26 mg/cm^2. The differences between the results were small (see Sec. V C).

The purpose of the simulation was to provide a coincidence matrix describing the relative detection probability as a function of the positron and electron energies corresponding to the hypothetical anomalous events (matrix **A**) and a matrix corresponding to Bhabha scattering (matrix **B**). For the analysis, the geometry of detection and the spectrometer resolution and response function must be taken into account (see Sec. III D).

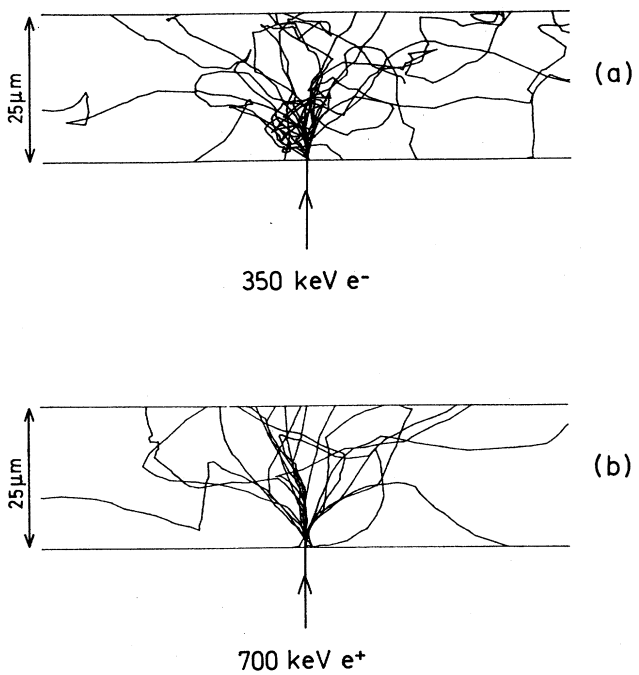

FIG. 2. Simulated trajectories for 350-keV electrons (a) and 700-keV positrons (b) normally incident on a 25-μm-thick thorium foil.

B. Simulating the anomalous events

A total of 50 000 electron-positron pairs were made to start from random positions in the thorium foil. For each pair, the initial energy of both particles was 350 keV. The initial direction of the positron was chosen at random, and the initial direction of the electron was required to be opposite to that of the positron. Both particles were followed through a multiple scattering and energy loss process until either leaving the source-target foil or being "absorbed" at a lower cutoff energy set to 100 keV. In the main run (with a 13-mg/cm^2 source layer), where a total of 10^5 particles started, 88.5% escaped from the foil. For geometry 1 and 2 the energy loss distribution had a FWHM of $\sim$40 keV for the particles emitted on the side without a source layer, and for geometry 3 a FWHM $\sim$80 keV for particles emitted on any of the sides. The angular distribution was somewhat peaked towards the normal [according to a distribution $\sim(\cos\theta)^{1.57}$]. The anomalous peak distribution, $\mathbf{A}(\varepsilon_+,\varepsilon_-)$ was computed for different initial electron (ε_-) and positron (ε_+) energies by translating the energy of the escaping electrons and positrons and applying the appropriate spectrometer profile function.

C. Simulating the Bhabha scattering

In the simulation of the **B** matrix, coincident electron-positron pairs were recorded if each of the two particles escaped from the source-target foil with an energy exceeding 200 keV. However, the probability for a Bhabha scattering event with an energy transfer larger than 200 keV is very small. For this reason, the following procedure was used. The primary positron, starting from the source layer, was followed through its scattering and energy loss process until either leaving the foil or reaching a lower cutoff energy of 400 keV. In this process, the probability for Bhabha events with energy transfer exceeding 200 keV was artificially increased (by a factor $\approx$300) to give on the average about one event per incident positron. Such artificial Bhabha events were recorded, but not allowed to affect the scattering history of the primary positron. For each generated Bhabha event, the scattered positron and electron were followed until one of the energies was below 200 keV.

Each run (e.g., the main run with a source layer thickness of 13 mg/cm^2) was based on a total number of 2×10^6 positrons starting from the source layer. Additional runs were performed for source layer mass thicknesses of 6.4 and 26 mg/cm^2.

D. Inclusion of geometry and spectrometer response

As described in Secs. III B and III C we obtained simulated data containing the direction and energy for each of a large number of coincident electron-positron pairs escaping from the source-target foil, pertaining to **A** and **B** matrix simulation, respectively. These data were pro-

cessed further to obtain coincidence matrices for the desired geometries and spectrometer settings.

The explored configurations, with the source side being the side covered by the source layer and the target side being the opposite side, were

Geometry 1: Positrons escaping on the target side and electrons on the source side.

Geometry 2: Electrons escaping on the target side and positrons on the source side.

Geometry 3: Electrons and positrons escaping on either side of the thorium target.

Geometry 4: Both particles escaping on the thorium target side.

In our measurements, geometries 1, 2, and 3 were used. Apparently, the measurements by Erb *et al.*[1] were made in geometry 4. Due to the asymmetry of the source-target foil, the different geometries lead to different coincidence spectra.

In geometries 1 and 2 the plane of the foil was perpendicular to the common symmetry axis of the lenses. Electrons and positrons were thus accepted within cones defined by $27.5° < \theta < 32.5°$, where θ is the angle relative to the normal of the foil surface. The spectrometer profile was assumed to be Gaussian with a momentum resolution of 7%. In geometry 3 the plane of the foil was parallel to the symmetry axis. Geometries 1 and 2 are here referred to as "transverse" geometries, while geometry 3 is referred to as "longitudinal".

The computed intensity of the anomalous peak is considerably larger (by a factor of ≈ 15) for the transverse geometries than for the longitudinal geometry. This can be understood from the previously mentioned angular distribution of escaping electrons and positrons. In the transverse geometry, electrons and positrons are detected at angles $\theta \approx 30°$ relative to the surface normal. In the longitudinal geometry, they are detected at somewhat varying θ, but $\theta \approx 70°$ may be a representative average. Since the solid angle is the same, the transverse signal should be related to the longitudinal approximately by the ratio

$$[(\cos 30°)^{1.57}/(\cos 70°)^{1.57}]^2 \approx 18 .$$

On the other hand, the "peak" in the **A** matrix is somewhat sharper in the longitudinal case. This can be understood as due to "anomalous events" occurring near the target surface, thus suffering small energy degradation. This feature is even more apparent for the geometry used by Erb *et al.*,[1] geometry 4. The energy degradation is demonstrated in Fig. 3, which shows the simulated coincidence positron spectrum for anomalous events detected in geometry 4. The result of the simulation shows a rather sharp peak with a FWHM of about 30 keV, a value which agrees well with the observations of Erb *et al.*

E. Simulation of electron scattering

The Møller background was calculated in a Monte Carlo simulation identical to the one described in Sec. III C, using the appropriate beta energy distributions for the electrons starting from the ^{90}Sr source and the Møller cross section for electron-electron collisions.

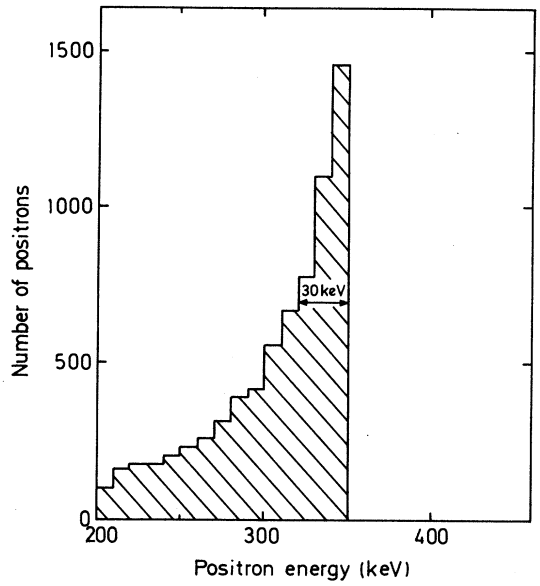

FIG. 3. Simulated coincidence positron spectrum for anomalous events detected in geometry 4 for an electron energy window 300–350 keV. The original electron and positron energies are 350 keV.

IV. ANALYSIS OF THE EXPERIMENTAL DATA

A. Positron scattering

The time difference between the electron and positron signals was registered. A typical time spectrum is shown in Fig. 4. A 3.6-ns wide window encompassing the peak containing "true" coincidences was placed slightly asymmetric relative to the peak maximum in accordance to the shape of the peak. A 72-ns-wide window containing chance coincidence events was also chosen.

For each source and each current-current combination, the coincidence events were entered into a pulse-height × pulse-height spectrum. Chance coincidences were subtracted point by point. Singles pulse-height spectra, taken at zero spectrometer current and at a current corresponding to a kinetic energy of 345 keV of the positrons are shown in Fig. 5. In the latter spectra the peak corresponds to a complete deposition of the particle kinetic energy. The shoulder above the peak in the spectrum from the positron detector corresponds to the additional energy deposited by one annihilation photon. The shape of the current-independent photon background contribution is seen in the spectrum obtained at zero current.

In order to select events corresponding to electron-positron coincidences, windows in the pulse-height × pulse-height spectrum encompassing the full-energy peaks were set. The position of the peak in the pulse-height spectra varies with the energy of the detected particle. In the previously presented analysis[11] we varied the position of the pulse-height window. However, for the present analysis we used a wider window with fixed position for all current settings. By this means the high-

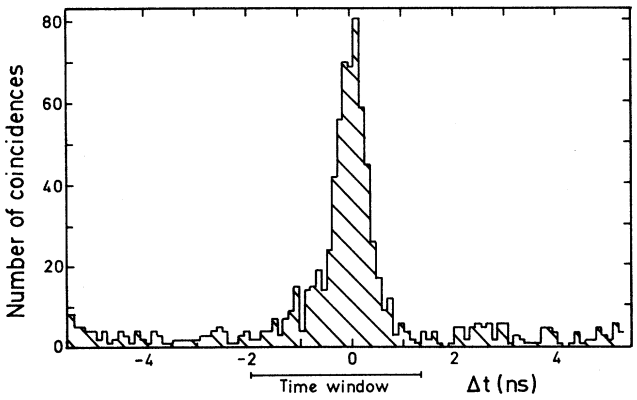

FIG. 4. The time difference between the electron and positron signals. The 3.6-ns time window used in the analysis for true coincidences is shown.

energy shoulder of the positron peak was included increasing the statistical precision. The analysis of the electron scattering showed this to be a reliable method, cf. Sec. V B.

There is a small background of positron-photon, electron-photon, and photon-photon coincidences. Figure 6(a) shows the positron pulse-height spectrum obtained in coincidence with a signal in the electron spectrometer corresponding to the correct electron pulse height. Figure 6(b) shows the positron pulse-height spectrum coincident with the photon background in the electron spectrometer. These background contributions were subtracted assuming no correlations in pulse height. The background was about 9% in geometry 1, 11% in geometry 2, and 18% in geometry 3.

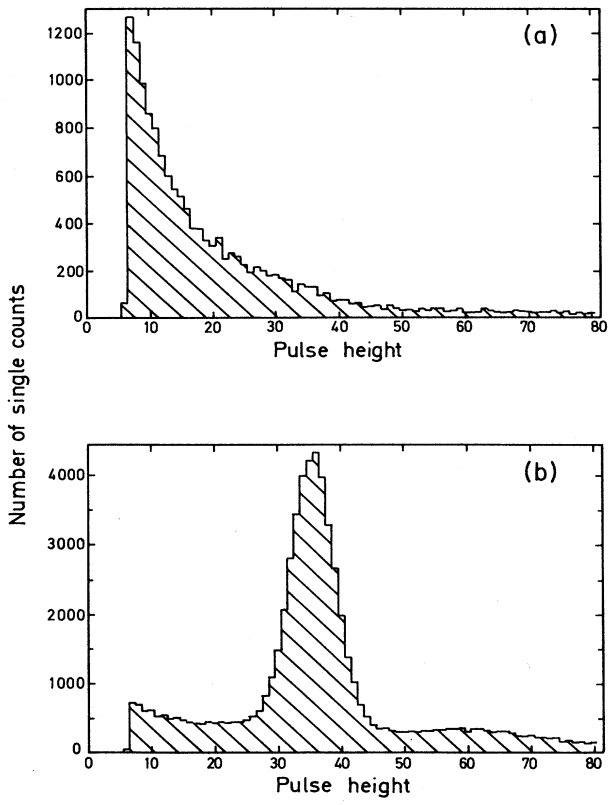

FIG. 5. Pulse-height spectrum shapes for positron single counts for (a) spectrometer setting corresponding to 0 keV and (b) spectrometer setting corresponding to 345 keV.

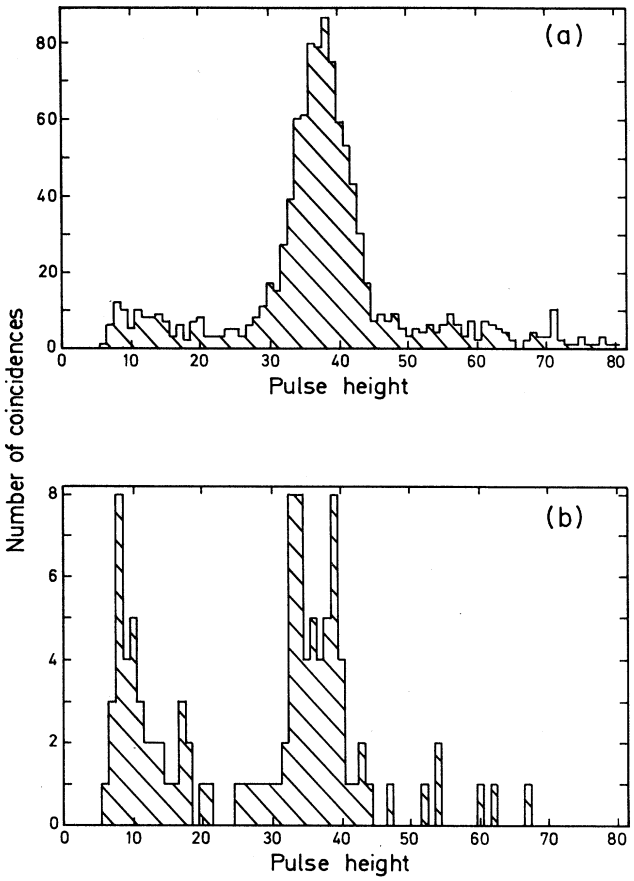

FIG. 6. Positron-pulse-height spectrum measured in coincidence with (a) the correct electron pulse-height interval and (b) an interval outside the correct electron pulse height, corresponding to the photon background. Both spectrometer settings correspond to 345 keV.

B. Electron scattering

The electron scattering data were treated in essentially the same way as the data on positron scattering. The width of the time windows used did, however, differ somewhat. The window containing true coincidences was 2.1 ns and the window for chance coincidences was 41-ns wide.

V. EXPERIMENTAL RESULTS

A. Positron scattering

The coincident electron and positron counting rates were measured for all combinations of the five different

positron and electron energies. The corrected number of counts was normalized to a constant source activity using the measured singles count rates. For each geometry, the normalized count rates for different sources were weighted together to form a 5×5 energy-energy coincidence matrix, $\mathbf{X}$.

The experimental data were analyzed under the assumption that they correspond to Bhabha scattering with a superimposed peak structure. The positron energy-electron energy distribution due to Bhabha scattering, calculated in the Monte Carlo simulation described in Sec. III C was smoothed by fitting to it a second order two-dimensional polynomial. The resulting matrix $\mathbf{B}$ was normalized to one positron starting from the source.

The positron energy-electron energy distribution associated with a resonance process in which a positron and electron are created, depends on the initial energies, ε_+ and ε_- after the decay of the resonance. The Monte Carlo simulated distribution due to such a process is contained in the matrix $\mathbf{A}(\varepsilon_+,\varepsilon_-)$, normalized to one electron-positron pair starting from within the thorium foil.

The expression $N(\mathbf{B}+C\cdot\mathbf{A}(\varepsilon_+,\varepsilon_-))$ was fitted to the experimental data $\mathbf{X}$, treating the overall normalization N, the peak contribution C, and the initial energies, ε_+ and ε_-, as unknown parameters. A maximum likelihood procedure was used for the fit. The experimental quantity

$$n_{ij}=X_{ij}(X_{ij}/\Delta X_{ij}^2)$$

was assumed to be Poisson distributed with a mean

$$\lambda_{ij}=N(B_{ij}+CA_{ij})(X_{ij}/\Delta X_{ij}^2)\ ,$$

i.e.,

$$\ln L=\sum n_{ij}\ln\lambda_{ij}-\lambda_{ij}$$

was maximized with respect to the unknown parameters. With no background corrections, n_{ij} equals the experimental number of counts.

In the analysis the initial energies were first assumed equal, $\varepsilon_+=\varepsilon_-=\varepsilon$, as suggested by the results of Erb *et al.*[1] The initial energy ε was allowed to vary in the interval 300–400 keV. Results of the fits to the data sets of the two transverse geometries and of a fit of the summed data set are shown in Fig. 7, where contours of the likelihood function at $2\ln L=2\ln L_{\max}-1$, $2\ln L_{\max}-4$, and $2\ln L_{\max}-9$ are shown. These contours correspond to one, two, and three standard deviations for one parameter, respectively. The resulting value of the peak contribution is $C_1=(13\pm7)\times10^{-6}$ and $C_2=(15\pm6)\times10^{-6}$. For the complete data set of the transverse geometries we obtain $C=(14\pm4)\times10^{-6}$. The corresponding initial energy is $\varepsilon_1=319\pm14$ keV and $\varepsilon_2=321\pm10$ keV and for the complete data set $\varepsilon=320\pm8$ keV.

The goodness of the fit can be expressed by the parameter

$$\Lambda=2(\ln L_0-\ln L_{\max})\ ,$$

where

$$\ln L_0=\sum n_{ij}\ln n_{ij}-n_{ij}\ ,$$

which corresponds to the minimum chi square in a least-squares fit. We obtain $\Lambda=30$ and $\Lambda=21$ for the two geometries, respectively, with 22 degrees of freedom. For the two data sets together we obtain $\Lambda=51$ with 46 degrees of freedom.

Figures 8 and 9 show the cross sections for geometries 1 and 2 as a function of the electron energy, summed over different positron energies. The full lines show the result of the fit including Bhabha scattering and an additional peak structure. For positron energies of 265 and 305 keV [Figs. 8(a) and 9(a)], the peak is seen to give a sizeable contribution, while for positron energies of 345, 385, and 425 keV [Figs. 8(b) and 9(b)], the data are well described by Bhabha scattering alone. In Figs. 8(a) and 9(a) the broken line shows the contribution from Bhabha scattering alone.

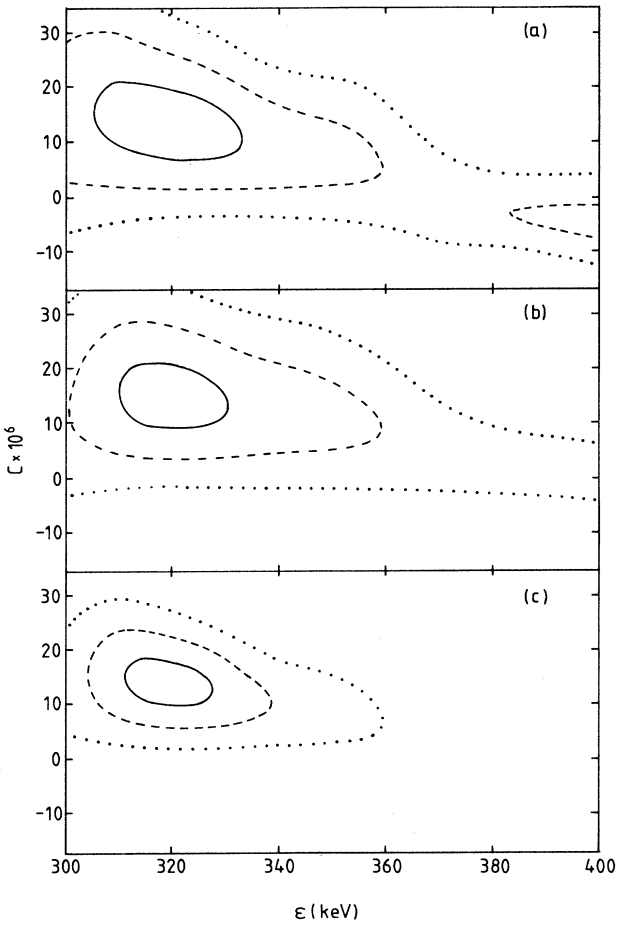

FIG. 7. Result of positron scattering. The results of the fit to the data of geometry 1 (a) and geometry 2 (b) and to the complete data set (c) under the assumption of equal energies for the produced electron and positron. The figure shows contours of the likelihood expression as a function of the peak contribution C and the initial energy of the electron and positron giving rise to the structure. The contours correspond to one (full line), two (broken line), and three (dotted line) standard deviations, respectively.

Repeating the analysis, but now allowing the initial energies of the electrons and positrons to vary independently, gives the result shown in Fig. 10 for the complete data set. This result agrees within one standard deviation with that obtained under the restriction $\varepsilon_+ = \varepsilon_-$.

We have also accumulated data in the longitudinal geometry (geometry 3). Because of the much more important effects of multiple scattering on any anomalous events originating from within the source-target foil, these data have not been included in the present analysis. However, the data have been used to exclude some possible interpretations of the results (cf. Sec. VI B).

B. Electron scattering

The analysis of the electron-electron coincidences was carried out in essentially the same way as the analysis for electron-positron coincidences described in Sec. V A.

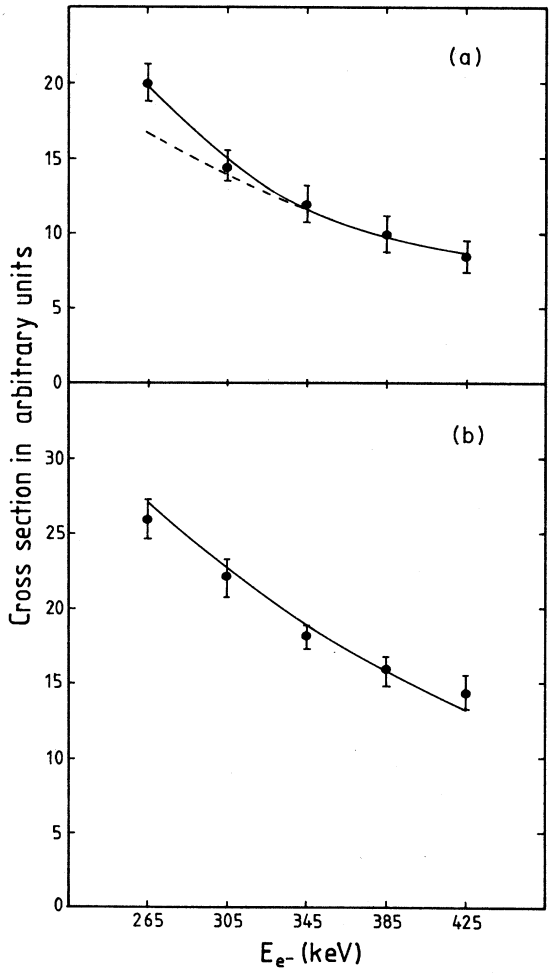

FIG. 8. The cross sections in arbitrary units for geometry 1 summed over the measured positron energies 265 and 305 keV (a) and 345, 385, and 425 keV (b). The full lines show the result of the fit including Bhabha scattering and an additional peak structure. The broken line shows the contribution of Bhabha scattering alone.

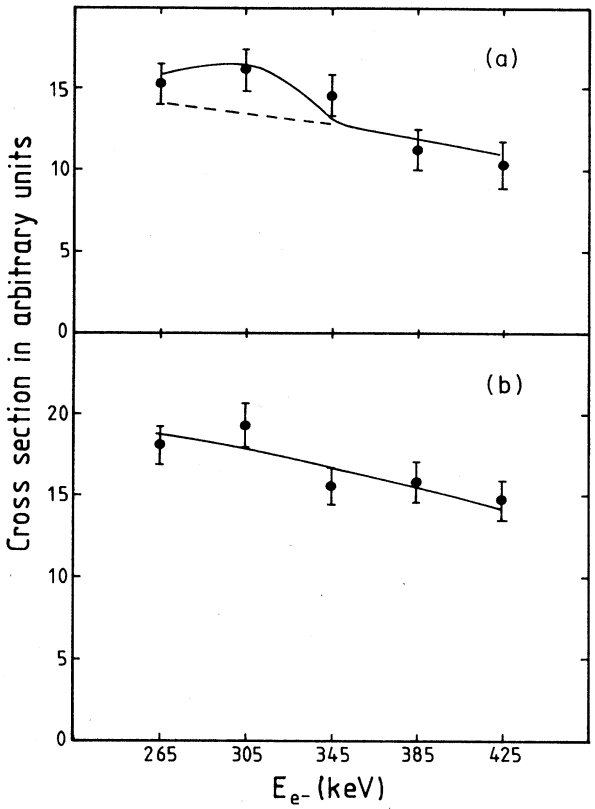

FIG. 9. The cross sections in arbitrary units for geometry 2 summed over the measured positron energies 265 and 305 keV (a) and 345, 385, and 425 keV (b). The full lines show the result of the fit including Bhabha scattering and an additional peak structure. The broken line shows the contribution of Bhabha scattering alone.

The coincidence data are supposed to originate mainly from Møller scattering. The spectra resulting from Møller scattering and subsequent scattering in the target foil were Monte Carlo simulated (cf. Sec. III) using the appropriate beta energy distributions for the electrons starting from the source. The data were analyzed with

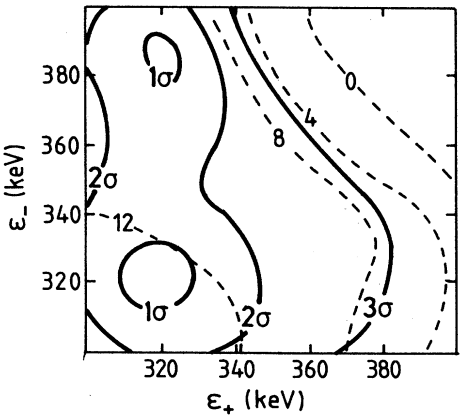

FIG. 10. The result of the fit to the complete data set without constraining the initial electron and positron energies. The full lines show the contours of the likelihood function corresponding to one, two, and three standard deviations. The broken lines show the resulting values for C in units of 10^{-6}.

various windows set in the pulse-height spectra. We expect a wide, current independent window to be least ambiguous and this procedure was used to extract the scattering data in the fit.

Maximum likelihood fits to the data, allowing for a peak of the same shape used for geometries 1 or 2 in the positron scattering case to be superimposed on the Møller background, do not result in any positive peaks. The quantity C describing the fitted peak component is shown in Fig. 11 as a function of the electron energy, assuming the energy of the two electrons to be equal. The best fits, resulting in $\Lambda = 15$ with 22 degrees of freedom for both of the distributions, correspond in fact to a slightly negative peak contribution. The value of Λ for a peak of the size and position obtained in the positron scattering case is 47 and 49 for geometries 1 and 2, respectively. The statistical probability that the peak energy and position are such that the value of Λ is greater than these values is completely negligible ($< 10^{-4}$).

The good agreement between the experimental and calculated energy distributions lends support to our use of current independent windows in the pulse-height spectra. This method of analysis was therefore also adopted in the analysis of the positron scattering data. Comparing the results for electron and positron scattering we conclude that it is very unlikely that the apparatus or the method of analysis is responsible for the structure observed in the positron scattering data.

C. Investigations of possible background effects

The spectral structure observed in positron scattering cannot be due to coincidences between positrons and Compton electrons, emanating from the positron detector and registered in the electron detector. The time difference between such coincident events should be approximately 2.5 ns larger than for positrons and electrons emanating from the source-target foil combination. The choice of the time window excludes such events. In Fig. 4 these events are expected at $\Delta t = 2.5$ ns, where a slight excess can be seen.

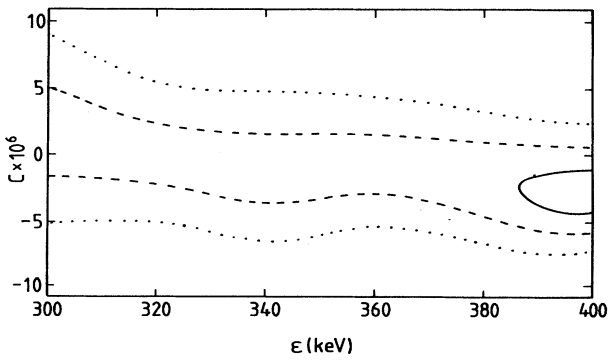

FIG. 11. Result of electron scattering. The contours of the likelihood expression as a function of the peak contribution C and the initial energy of any of the produced electrons, assumed to be equal. The contours correspond to one (full line), two (broken line), and three (dotted line) standard deviations.

We have investigated the possibility that positron annihilation and Compton scattering in the target produce two electrons which both reach the detectors. For a conservative estimate we assume all the detected electrons to be Compton electrons originating from the annihilation process. The probability for an electron to pass through the positron spectrometer is taken to be 10^{-3}.[15] We find the coincidence rate to be less than 10^{-3} of the measured rate. An effect not included in this estimate is electrons ejected by the annihilation quanta in the baffles and other parts of the spectrometer. The importance of this process has been evaluated by measuring electron-electron coincidences with a ^{22}Na positron source in the spectrometer. Also in this case the resulting upper limit is several orders of magnitude smaller than the observed effect. Thus, we can rule out that coincident electrons are the cause of the measured anomalous structure.

Photon-photon coincidences due to positron annihilation in the vicinity of the source are removed by the background subtraction. Further, since this background is current independent, it is present to an equal amount in all current-current combinations. In fact, analyzing data sets obtained with no cuts in pulse heights gave no significant changes in the results of the fits. Other possible sources of systematic effects were investigated. Analyzing the data with independent overall normalizations for each source did not alter our conclusions.

The results were also almost insensitive to changing the source thickness assumed in the Monte Carlo simulations to be between 6.5 and 26 mg/cm^2. The estimated electron and positron energies at the possible anomalous structure varied with about 10 keV, being lower for the simulation with the thinner source thickness and higher for the simulation with the thicker one. The significance of the peak structure was practically constant for the different source thicknesses.

D. Derivation of the peak cross section

The cross section for the anomalous peak structure (σ_A) can be estimated from the observed probability of an anomalous event per source positron (C), the width of the peak (ΔE), the stopping power of the target (S) and the probability that an arbitrary positron starting from the source will reach the appropriate energy in the thorium foil (P). The Monte Carlo simulations show this probability P to be 2.6%. When the positron energy is within the correct energy interval ΔE, the mean free path for the anomalous event to occur is $1/n\sigma_A$, where n is the number of electrons per unit volume. The distance covered by the positron having an energy in the interval defined by ΔE is $\Delta E/S$, resulting in a peak cross section expressed as

$$\sigma_A \cdot \Delta E = CS/Pn \ .$$

With a measured value of the peak contribution of $(14 \pm 4) \times 10^{-6}$ (parameter C in Sec. V A), the peak cross section

$$\sigma_A \cdot \Delta E = (1.9 \pm 0.6) \times 10^3 \text{ mb keV} \ ,$$

where ΔE is the real width of the peak structure.

VI. POSSIBLE EXPLANATIONS OF THE PEAK STRUCTURE

A. Introduction

As seen in Sec. V, the experimental results show the possible presence of a peak structure in the coincident electron and positron energy spectra. We briefly discuss some proposed explanations for coincident electron positron peaks in positron-electron scattering experiments, in which the electron is residing in a heavy element (like thorium in our case). As it has been suggested that the effects seen in heavy-ion collisions and positron scattering might have a common origin, we also briefly comment on the heavy-ion results.

B. The new particle explanation

In the longitudinal geometry (geometry 3) the geometrical acceptance is approximately 50 times larger for the decay of a slowly moving particle into an electron-positron pair outside the source-target foil. In this case the secondary electron and positron are unaffected by the strong Coulomb field close to the heavy nucleus and (for the most part) by multiple scattering in the foil. From the data collected in the longitudinal geometry, we can exclude that the effect present in the data taken in the transverse geometries is due to a particle decaying into a back-to-back electron and positron just outside the target foil.

Moreover, the results of our experiment and that of Erb *et al.* are very difficult to explain as being due to a particle which is produced in an elementary e^+-e^- process and then decaying to an electron-positron pair. The reason is that the laboratory motion of the produced object would be large enough to smear the peak since an isotropic decay into e^+e^- in the rest frame would be boosted to a flat kinetic energy distribution of the leptons in the laboratory system. Thus, the most one would see is an edge, not monoenergetic peaks of the same energy for both the electrons and positrons.

Evidence against an elementary particle interpretation of the coincident electron-positron peaks also comes from investigation of rare decays of known particles as the new particle would affect the decay rate due to the virtual intermediate states. The combined constraints from the nonobservation of light particles coupling to electrons and positrons in the decays $K^+ \to \pi^+ e^+ e^-$, $\pi^+ \to \nu 3e$, $\Sigma^+ \to p e^+ e^-$, $B \to K e^+ e^-$, and nuclear $\Delta T = 0$ transitions rule out particles coupling to any of the known quarks of the strength needed to explain the observed heavy nucleus results.[13] The additional constraints from the electron $g-2$ measurements and the particle searches in different electron beam dump experiments rule out short-lived elementary particles coupling only to electrons.

One way to explain the possible structure observed in the coincident electron positron spectrum would be if there is an excitation produced practically at rest in the field of the nucleus and which then slowly moves out far enough from the nucleus before decaying to avoid shifting of the kinetic energies due to the strong Coulomb fields. However, we are unable to provide the physical mechanism needed for such a scenario.

C. The new QED phase explanation

An important aspect of spontaneously broken symmetries is the fact that particles propagating through the new, true vacuum may have quite different properties than in the symmetric phase. If there would be a new phase of QED in the presence of strong fields, even the properties of bound states such as positronium could in principle change. Speculations of the existence of a new phase of QED have been advocated[20] primarily to explain the results of the heavy-ion experiments mentioned earlier. In Ref. 21, however, the authors argue that there is no good theoretical indication of a new phase of QED caused by strong, but weakly varying electric fields. The main argument is that also for large electromagnetic fields the smallness of the coupling constant $\alpha = \frac{1}{137}$ will make these effects small.

D. Conclusions concerning possible explanations

The interpretation of the narrow peak observed by Erb *et al.* as well as our results obtained with the transverse geometry in terms of a particle decaying into monoenergetic electrons and positrons, has great difficulties. The interpretation of the effect as a slowly moving particle decaying just outside the target is contradicted by our results with the longitudinal geometry run. Also other investigations, like the study of rare decays of known particles and the electron $g-2$ measurements rule out the necessary coupling strengths of an elementary particle to quarks and leptons in order to explain the results of the heavy-ion and the positron scattering experiments, respectively.

The interpretation of the observed effects in terms of a new QED phase in the presence of a strong electric field seems primarily to suffer from theoretical shortcomings. We conclude that at present all models fall short of explaining the observed features in heavy-ion reactions and positron collisions. It should be mentioned that the experiments under discussion are generally difficult to perform and that particularly for the positron scattering experiments there are conflicting results.

VII. CONCLUSIONS

We have investigated the structure of coincidence spectra resulting from scattering of low-energy positrons and electrons on thorium targets. The coincidence spectra are markedly different for the two kinds of particles falling on the target. No peak was discerned in the electron spectra resulting from electron scattering. The same apparatus and method of analysis were used in the study of positron scattering.[11] We conclude that no instrumental effects or other flaws in the method used are the source of the peak structure observed in positron scattering.

The work we present in this paper strengthens the conclusion drawn previously. The electron and positron spectra resulting from positron scattering on thorium are

best described in terms of Bhabha scattering with a small additional structure at an energy of about 320 keV for both electrons and positrons. The intrinsic width of this structure is less than 40 keV, our experimental energy resolution. We find the effect to be three standard deviations from zero. Anomalous effects in the same energy region have been reported by Erb[1] and Sakai *et al.*[8]

At these energies the effects of multiple scattering are very large. These effects show up in the rather different experimental results obtained for the different source-target geometries. These differences are well reproduced by the Monte Carlo simulations. We are unable to explain the observed anomalous spectra structures in terms of conventional physics. This makes it important to further explore this type of process.

ACKNOWLEDGMENTS

We are grateful to Mrs. P. Federman for preparing the sources and thank L. Eriksson and the staff at Karolinska Hospital for giving us access to their gallium generator. Our thanks also go to L. Bergström and H. Rubinstein. The discussion of the possible theoretical explanations would have been difficult without their keen participation. We also thank M. Ismail for useful discussions and assistance. This work was supported by the Swedish Natural Science Research Council.

[1]K. A. Erb, I. Y. Lee, and W. T. Milner, Phys. Lett. B **181**, 52 (1986).

[2]R. Peckhaus, Th.W. Elze, Th. Rapp, and Th. Dresel, Phys. Rev. C **36**, 83 (1987).

[3]T. F. Wang, I. Ahmad, S. J. Freedman, R. V. F. Janssens, and J. P. Schiffer, Phys. Rev. C **36**, 2136 (1987).

[4]K. Maier, E. Widmann, W. Bauer, F. Bosch, J. Braggmann, H.-D. Carstanjen, W. Decker, J. Diehl, R. Feldmann, B. Keyerleber, D. Maden, J. Major, H.-E. Schaefer, A. Seeger, and H. Stoll, Z. Phys. A **330**, 173 (1988).

[5]H. Tsertos, C. Kozhuharov, P. Armbruster, P. Kienle, B. Krusche, and K. Schreckenbach, Z. Phys. A **331**, 103 (1988); Phys. Lett. B **207**, 273 (1988).

[6]E. Lorenz, G. Mageras, U. Stiegler, I. Huszar, Max-Planck-Institut für Physik und Astrophysik Report MPI-PAE/Exp. E1 190.

[7]J. van Klinken, W. J. Meiring, F. W. N. de Boer, S. J. Schaafsma, V. A. Wichers, S. Y. van der Werf, G. C. Th. Wierda, H. W. Wilshut, and H. Bokemeyer, Phys. Lett. B **205**, 223 (1988).

[8]M. Sakai, Y. Fujita, M. Imamura, K. Omata, S. Ohya, and T. Miura, Phys. Rev. C **38**, 1971 (1988).

[9]J. Schweppe, A. Gruppe, K. Bethge, H. Bokemeyer, T. Cowan, H. Folger, J. S. Greenberg, H. Grein, S. Ito, R. Schule, D. Schwalm, K. E. Stiebing, N. Trautmann, P. Vincent, and M. Waldschmidt, Phys. Rev. Lett. **51**, 2261 (1983); M. Clemente, E. Berdermann, P. Kienle, H. Tsertos, W. Wagner, C. Kozhuharov, F. Bosch, and W. Koenig, Phys. Lett. **137B**, 41 (1984); T. Cowan, H. Backe, K. Bethge, H. Bokemeyer, H. Folger, J. S. Greenberg, K. Sakaguchi, D. Schwalm, J. Schweppe, K. E. Stiebing, and P. Vincent, Phys. Rev. Lett. **56**, 444 (1986); P. Kienle, Annu. Rev. Nucl. Part. Sci. **36**, 605 (1986).

[10]K. Danzmann, W. E. Meyerhof, E. C. Montenegro, Xiang-Yuan Xu, E. Dillard, H. P. Hülskotter, F. S. Stephens, R. M. Diamond, M. A. Deleplanque, A. O. Macchiavelli, J. Schweppe, R. J. McDonald, B. S. Rude, and J. D. Molitoris, Phys. Rev. Lett. **59**, 1885 (1987).

[11]Chr. Bargholtz, L. Holmberg, K. E. Johansson, D. Liljequist, P.-E. Tegnér, L. Bergström, and H. Rubinstein, J. Phys. G **13**, L265 (1987).

[12]J. E. Kim, Phys. Rep. **150**, 1 (1987).

[13]R. D. Peccei and H. R. Quinn, Phys. Rev. Lett. **38**, 1440 (1977); S. Weinberg, *ibid.* **40**, 223 (1978); F. Wilczek, *ibid.* **40**, 279 (1978).

[14]W. A. Bardeen, R. D. Peccei and T. Yanagida, Nucl. Phys. **B279**, 401 (1987).

[15]T. R. Gerholm and J. Lindskog, Ark. Fys. **24**, 171 (1963).

[16]R. E. Ekström and T. Arctaedius, Nucl. Instrum. Methods, **A252**, 125 (1986).

[17]M. Ismail and D. Liljequist, University of Stockholm, Department of Physics USIP Report 86-11, 1986.

[18]Nucl. Data Sheets **33**, 481 (1981).

[19]D. Liljequist and M. Ismail, J. Appl. Phys. **62**, 342 (1987).

[20]L. S. Celenza, V. K. Mishra, C. M. Shakin, and K. F. Liu, Phys. Rev. Lett. **57**, 55 (1986).

[21]R. D. Peccei, J. Sola, and C. Wetterich, Phys. Rev. D **37**, 2492 (1988).